Power Electronic Systems
Laboratory

IEEE Transactions on Components, Packaging, and Manufacturing Technology, Vol. 1, No. 4, pp. 528-535, April 2011.

Analysis of Theoretical Limits of Forced-Air Cooling Using Advanced Composite Materials with High Thermal Conductivities

U. Drofenik
A. Stupar
J. W. Kolar

Eidgenössische Technische Hochschule Zürich
Swiss Federal Institute of Technology Zurich

Analysis of Theoretical Limits of Forced-Air Cooling Using Advanced Composite Materials with High Thermal Conductivities

Uwe Drofenik, *Member, IEEE,* Andrija Stupar, *Student Member, IEEE,* and Johann W. Kolar, *Fellow, IEEE*

***Abstract*—Cooling systems take a significant portion of the total mass and/or volume of power electronic systems. In order to design a converter with high power density, it is necessary to minimize the converter's cooling system volume for a given maximum tolerable thermal resistance. This paper theoretically investigates whether the cooling system volume can be significantly reduced by employing new advanced composite materials like isotropic aluminum/diamond composites or anisotropic highly orientated pyrolytic graphite. Another strategy to improve the power density of the cooling system is to increase the rotating speed and/or the diameter of the fan, which is limited by increasing power consumption of the fan. Fan scaling laws are employed in order to describe volume and thermal resistance of an optimized cooling system (fan plus heat sink), resulting in a single compact equation dependent on just two design parameters. Based on this equation, a deep insight into different design strategies and their general potentials is possible. The theory of the design process is verified experimentally for cooling a 10 kW converter. Further experimental results showing the result of the operation of the optimized heat sink are also presented.**

***Index Terms*—Cooling systems, heat sink optimization, power density, power electronic systems.**

I. Introduction

POWER ELECTRONIC converters are essential system components wherever electricity has to be provided. There is a strong desire to continuously increase the power density of converter systems to ease their integration into larger systems and products. Since the cooling system of a converter is typically a significant contributor to its volume and weight, therefore, in this paper we investigate the theoretical limits of minimizing the volume of a forced-air convective cooling system composed of fan and heat sink for a desired thermal resistance.

Research recent and past has been devoted to heat sink optimization [1]–[5]. An optimized heat sink, that is, a heat sink plus fan system, suited for a particular application, can do much in terms of reducing overall volume [2]. Alternatively and/or additionally the fan power can be increased to improve the convective cooling. The optimization procedure used for the purpose of this paper is that described in [2]. Basically, the optimization can be explained like this: for a heat sink channel with a certain length, there results a certain pressure drop along the channel in the direction of the air flow. Balancing this pressure drop against the fan pressure gives the operating point of the fan. Increasing the length of the heat sink will increase the pressure drop and reduce the air flow volume, but on the other hand increase the total fin surface employed for convective cooling. Here, an optimum heat sink length concerning minimum thermal resistance of the heat sink can be found. An important side condition is the minimum base plate area A_{CHIP} needed for placing the power chips of the converter. For each fin there is a certain minimum fin thickness necessary to transport an optimum amount of heat to the fin surface.

The question of flow bypass treated in [5] and [6] is not considered here since this phenomenon can be avoided with proper channelling of the air from the fan.

A further very interesting development is the recent introduction of new materials providing extremely high thermal conductivity [7]–[12] (see Table I), that theoretically might be employed as heat sink material. In this paper, we investigate if it makes sense to consider employing such advanced materials for the manufacture of heat sinks, and what performance improvements might be possible. As noted earlier, since there is for each heat sink fin a minimum thickness required for the transport of an optimum amount of heat to its surface, If the thermal conductivity of the fin material is increased, thinner fins can be employed, which means that the number of fins can be increased resulting in a larger total fin surface, and, therefore, improved convective heat transfer [1], [2]. Since all these effects are highly non-linear, we cannot simply assume that, for example, doubling the thermal conductivity of the material will reduce the thermal resistance of the heat sink by a factor of two. It is necessary to obtain an analytical description of this heat transfer problem based on empirical expressions, and then to perform a systematic optimization. The question of manufacturing such heat sinks and fans, of their reliable operation and of the costs is excluded from this paper, and is treated elsewhere [13]. Although this investigation is mainly theoretical, we discuss practical aspects in Section III, and give experimental data of prototype heat sinks optimized according to the theory presented here in order to verify our underlying mathematical models.

Manuscript received August 31, 2009; revised May 6, 2010; accepted September 5, 2010. Date of publication March 7, 2011; date of current version April 8, 2011. Recommended for publication by Associate Editor J. J. Liu upon evaluation of reviewers' comments.

The authors are with the Swiss Federal Institute of Technology Zurich, Zurich 8006, Switzerland (e-mail: drofenik@lem.ee.ethz.ch; stupar@lem.ee.ethz.ch; kolar@lem.ee.ethz.ch).

Color versions of one or more of the figures in this paper are available online at http://ieeexplore.ieee.org.

Digital Object Identifier 10.1109/TCPMT.2010.2100730

TABLE I
PROPERTIES OF THERMAL MATERIALS [7]–[12]

Material	Thermal Conductivity (W/mK)	In-Plane Coef. of Therm. Exp. (ppm/K)	Specific Weight (kg/m^3)
Aluminum	210 (isotr.)	23	2700
Copper	380 (isotr.)	17	8930
Diamond	2200 (isotr.)	2	3500
Natural graphite in epoxy-matrix	370 (xy)/6.5 (z-dir.)	−2.4	1940
Continuous carbon fibers in SiC-matrix	370 (xy)/38 (z-dir.)	2.5	2200
Diamond particles in Al-matrix	650 (isotr.)	7	3100
Highly orientated pyrolytic graphite	1700 (xy)/20 (z-dir.)	8	2250

II. OPTIMIZATION OF COOLING SYSTEM DESIGN

A. Detailed Optimization Procedure

Based on empirical and analytical expressions, the air flow and the resulting thermal resistance of the heat sink can be calculated as performed in the following. A detailed description of the mathematical procedure and (1)–(14), and the accuracy of the theory, verified by experimental results, can be found in [2], [14], and [15]. The investigation is limited to the heat sink shape shown in Fig. 1

$$k = \frac{s}{b/n} \tag{1}$$

$$d_h = \frac{2s \cdot c}{s + c} \tag{2}$$

$$\Delta p_{lam}(V) = \frac{48\,\rho_{AIR}\,\nu_{AIR}\,L}{n\,(s \cdot c)\,d_h^2}\;\; V \tag{3}$$

$$\Delta p_{turb}(V) = \frac{L\,\frac{s+c}{2s \cdot c}\;\rho_{AIR}\;\frac{1}{2}\left(\frac{V}{n\,(s \cdot c)}\right)^2}{\left(0.79 \cdot \ln\left(\frac{2V}{n\,(s+c)\,\nu_{AIR}}\right) - 1.64\right)^2} \tag{4}$$

$$Re_m = \frac{2\,V}{n\,(s + c)\,\nu_{AIR}} \tag{5}$$

$$k \cdot \Delta p_{FAN}\,(V) = \Delta p_{lam}(V_{lam}) \;\rightarrow\; V_{lam} \;\rightarrow\; Re_{m,lam} < 2300\;? \tag{6}$$

$$Nu_{m,lam} = \frac{3.657\;\left[\tanh\;\left(2.264X^{1/3} + 1.7X^{2/3}\right)\right]^{-1} + \frac{0.0499}{X}\;\tanh\,(X)}{\tanh\,\left[2.432\;Pr^{1/6}X^{1/6}\right]} \tag{7}$$

$$X = \frac{L}{d_h\,Re_m\,Pr} \tag{8}$$

$$Nu_{m,turb} = \frac{\{8 \cdot (0.79 \cdot \ln\,(Re_m) - 1.64)^2)\}^{-1}\,(Re_m - 1000)\;Pr}{1 + 12.7\,\sqrt{\{8 \cdot (0.79 \cdot \ln\,(Re_m) - 1.64)^2)\}^{-1}}\,(Pr^{2/3} - 1)} \cdot \left(1 + \left(\frac{d_h}{L}\right)^{2/3}\right). \tag{9}$$

k	fin spacing ratio
λ_{HS} (W/mK)	thermal conductivity of heat sink material
A_{HS} (m^2)	size of the heat sink base plate
d_h (m)	hydraulic diameter of one channel
L (m)	channel length in air flow direction
n	number of channels
Δp (N/m^2)	pressure drop in one channel
V (m^3/s)	volume flow
Re_m	avg. Reynolds number (for lam. or turb. flow)
Nu_m	avg. Nusselt number (for lam. or turb. flow)
h (W/m^{2}K)	(convective) heat transfer coefficient
$Pr \approx 0.71$	Prandtl number (air, 80°C)
$\rho_{AIR} \approx 0.99$ (kg/m^3)	air density (80°C)
$\nu_{AIR} \approx 2.1\text{e-}5$ (m^2/s)	kinematic viscosity of the air (80°C)
$c_{p,AIR} \approx 1010$ (J/kgK)	specific thermal capacitance of air
$\lambda_{AIR} \approx 0.03$ (W/mK)	thermal conductivity of air (80°C)

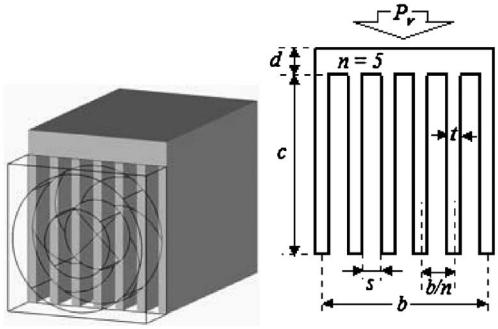

Fig. 1. Geometry of the heat sink investigated in this paper. In order to provide the whole fin surface with air flow, the heat sink dimensions have to match the fan size resulting in $b = c = D$, where D is the diameter of the fan facing the heat sink. Thermal losses P_V (W) occur at the top of the base plate and are homogenously distributed over the area $A_{CHIP} = b \cdot L$.

The procedure of obtaining the pressure in one channel (3)–(6) is shown graphically in Fig. 2. Employing (6), it is decided if the flow problem is laminar or turbulent. With empirical equations (7)–(9) the convective heat transfer is defined. Finally, employing the model of Fig. 3, the thermal resistance of the heat sink can be calculated via (10)–(14). The nonlinear equations (1)–(14) can be easily solved numerically [2], but due to their complexity, it is very difficult to gain insight into the relationships between various design parameters like fan speed, fan diameter, thermal conductivity of the heat sink material, total chip area, or heat sink length

$$h = \frac{Nu_m \cdot \lambda_{AIR}}{d_h} \tag{10}$$

$$R_{th,A} = \frac{1}{h \cdot L \cdot c} \tag{11}$$

$$R_{th,FIN} = \frac{\frac{1}{2}c}{\frac{1}{2}t \cdot L \cdot \lambda_{HS}} \tag{12}$$

$$R_{th,d} = \frac{d}{\frac{1}{n}A_{HS}\lambda_{HS}} \tag{13}$$

$$R_{th,S-a}^{(HS)} = \frac{1}{n}\left(R_{th,d} + \frac{1}{2}\left(R_{th,FIN} + R_{th,A}\right)\right) + \frac{0.5}{\rho_{AIR}\,c_{P,AIR}\;V}. \tag{14}$$

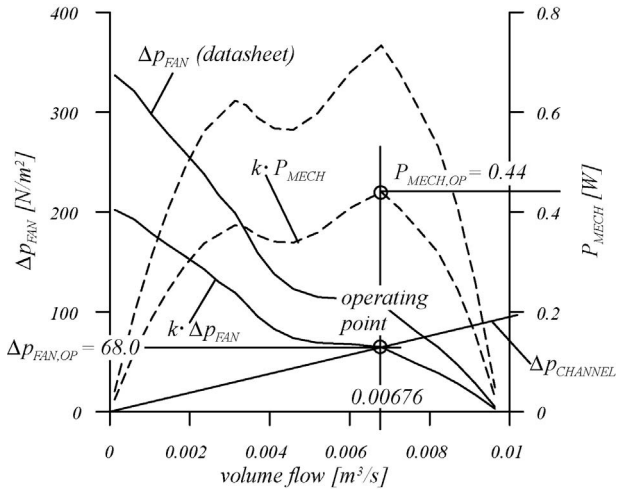

Fig. 2. Fan characteristic of SanAce 40 × 40 × 28/50dB [16] showing fan pressure Δp_{FAN} dependent on the air flow V (m^3/s). To calculate the fan operating point, Δp_{FAN} has to be multiplied with the fin spacing ration k. The heat sink channel pressure drop $Dp_{CHANNEL}$ is shown for laminar flow in linear dependency of the flow. Intersection of the two characteristics gives the fan operating point which is for optimized heat sinks typically (but not necessarily!) close to the maximum "mechanical power" of the air flow.

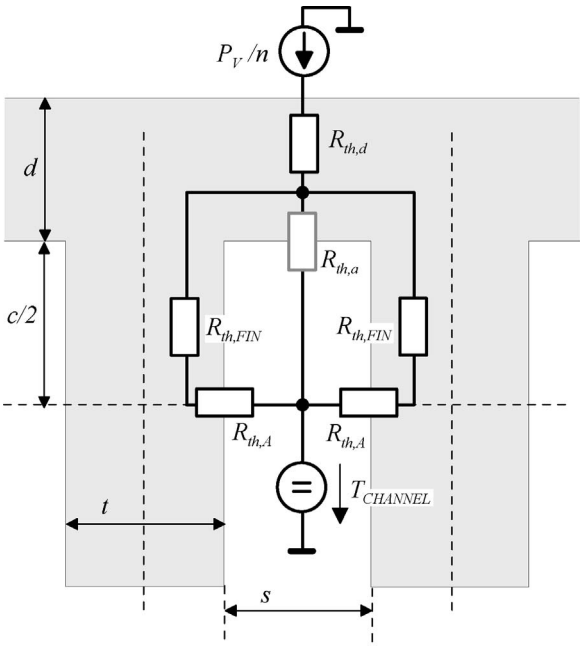

Fig. 3. Thermal network used to describe the heat transfer from heat sink surface (location of the power modules, i.e., chips) into the air flowing through a channel of the heat sink.

B. Analyzing the Different Contributions to the Thermal Resistance of the Heat Sink

With some general assumptions, (1)–(14) can be significantly simplified. The simplified equations as presented in the following are not useful to meet specific design targets, like a certain surface-to-air thermal resistance $R_{th,S\text{-}a}{}^{(HS)}$ of the heat sink, with very high accuracy, but do clearly show what kind of design parameters influence the system on what scale. The merit of certain optimization strategies like increasing the fan rotating speed, changing the geometric design of the heat sink, or increasing the thermal conductivity of the heat sink material can be seen much more clearly.

The first assumptions for deriving the simplified equations are that we operate the fan close to the maximum mechanical power, and that maximum fan pressure $\Delta p_{F,MAX}$ is reduced by approximately 50% [factor of 0.5 in (16)] due to the partial air flow from the fan facing not channels but fins [9]. Since for typical fans the maximum mechanical power is shifted from the symmetric center to the right (see Fig. 2), we can roughly approximate maximum air flow and pressure, respectively, as

$$V_{MAX} \approx \tfrac{2}{3} \cdot V_{F,MAX} \tag{15}$$

$$\Delta p_{MAX} \approx \tfrac{1}{3} \cdot 0.5 \cdot \Delta p_{F,MAX}. \tag{16}$$

This is also a fan operating area that is often recommended in fan datasheets. Our second assumption is that the number of fins is larger than at least 5, so that we can write

$$s << c \quad \rightarrow \quad d_h \approx 2s. \tag{17}$$

The third assumption is laminar or mixed flow in the operating point. As we experienced in various optimizations [2], the optimized operating point is very often in the vicinity of the boundary region between laminar and turbulent flow ("mixed flow"), where the laminar equations are still a very good approximation. From (3) we get

$$\frac{s^3 n\, c}{L} = 48 \cdot \rho_{AIR} \nu_{AIR} \frac{V_{F,MAX}}{\Delta p_{F,MAX}} \approx 10^{-3} \frac{V_{F,MAX}}{\Delta p_{F,MAX}} \tag{18}$$

which defines the condition of operating the fan close to its maximum mechanical power. Then, the fin thickness can be calculated as

$$t = \frac{c}{n} - s \approx s \cdot \left[10^3 \cdot \frac{\Delta p_{F,MAX}}{V_{F,MAX}} \cdot \frac{s^2 c^2}{L} - 1 \right] \tag{19}$$

which must not be negative, resulting in the condition

$$s > \sqrt{10^{-3} \cdot \frac{V_{F,MAX}}{\Delta p_{F,MAX}} \cdot \frac{L}{c^2}}. \tag{20}$$

In (17) we assume a minimum fin number of 5, resulting in the second condition for the channel thickness s as

$$\begin{aligned} n &= 10^{-3} \cdot \frac{V_{F,MAX}}{\Delta p_{F,MAX}} \cdot \frac{L}{s^3 c} \\ &\geq 5 \rightarrow s \leq \sqrt[3]{\tfrac{1}{5} \cdot 10^{-3} \cdot \frac{V_{F,MAX}}{\Delta p_{F,MAX}} \cdot \frac{L}{c}}. \end{aligned} \tag{21}$$

As can be seen in (14), the thermal resistance of the heat sink $R_{th,S\text{-}a}{}^{(HS)}$ is composed of three components: the conductive resistance of the sink material $R_{th,FIN}$ mainly through the fins, a convective resistance $R_{th,conv}$ from fin surface into the air, and a resistance $R_{th,\Delta T}$ due to the temperature rise of the air flowing from channel inlet to channel outlet

$$R_{th,S-a}^{(HS)} = R_{th,FIN}^{*} + R_{th,conv} + R_{th,\Delta T} \tag{22}$$

$$\begin{aligned} R_{th,FIN}^{*} &= \tfrac{1}{n} R_{th,d} + \tfrac{1}{2n} R_{th,FIN} \approx \tfrac{1}{2n} R_{th,FIN} = \tfrac{c}{2n\, \lambda_{HS} L\, t} \\ &= \tfrac{1}{2\lambda_{HS} L} \cdot \tfrac{1}{1 - 10^{-3} \cdot \frac{V_{F,MAX}}{\Delta p_{F,MAX}} \cdot \frac{L}{s^2 c^2}}. \end{aligned} \tag{23}$$

The equation of the laminar Nusselt number (7) can be approximated as

$$Nu_{m,lam} \approx 2.7 \cdot \left[1 + \frac{1}{4.5 \cdot \sqrt{X}}\right] \tag{24}$$

with

$$X \approx \frac{3\,\nu_{AIR}}{8\,Pr} \cdot \frac{L\,n\,c}{V_{F,MAX}} \tag{25}$$

resulting in

$$Nu_{m,lam} \approx 2.7 \cdot \left[1 + 66.7 \cdot \sqrt{V_{F,MAX}\frac{s}{L\,n\,c}}\right]. \tag{26}$$

Based on this and employing (11), (17), and (18), the convective resistance is given as

$$\begin{aligned} R_{th,conv} &= \tfrac{1}{2n} \cdot \frac{2s}{L\,c\,\lambda_{AIR} Nu_{m,lam}} \\ &\approx \frac{1.3 \cdot 10^4 \cdot \frac{\Delta p_{F,MAX}}{V_{F,MAX}} \cdot \frac{s^4}{L^2}}{1 + 2 \cdot 10^3 \cdot \sqrt{\Delta p_{F,MAX}} \cdot \frac{s^2}{L}}. \end{aligned} \tag{27}$$

Finally, the third resistive component is calculated as

$$R_{th,\Delta T} = \frac{0.5}{\rho_{AIR}\,c_{p,AIR} \cdot \frac{2}{3} V_{F,MAX}} \approx \frac{7.5 \cdot 10^{-4}}{V_{F,MAX}}. \tag{28}$$

C. Influence of the Fan

Maximum air flow rate $V_{F,MAX}$ (m^3/s), maximum pressure $\Delta p_{F,MAX}$ (N/m^2), input power P_{FAN} (W), and noise $noise_{FAN}$ (dB) of a fan are dependent [17] on rotating speed N (rpm) and diameter D (m) as described by

$$V_{F,MAX} = k_1 \cdot N \cdot D^3 \tag{29}$$

$$\Delta p_{F,MAX} = k_2 \cdot N^2 \cdot D^2 \tag{30}$$

$$P_{FAN} = k_3 \cdot N^3 \cdot D^5 \tag{31}$$

$$noise_{FAN} \propto \log(N). \tag{32}$$

Based on datasheet information [16], we investigated 65 commercially available fans for electronics cooling. The fan diameters varied from 40 mm to 200 mm (factor 5), the rated power varied between 0.5 W and 25 W (factor 50), and the rated fan speed between 1700 rpm and 15500 rpm (variation factor 9). Using the simple laws (29)–(31), we calculated the parameters k_1, k_2, k_3 for these 65 fans as

$$k_1 = \left[6.0 \cdot 10^{-3} \ldots 13.5 \cdot 10^{-3}\right] \tag{33}$$

$$k_2 = \left[3.94 \cdot 10^{-4} \ldots 8.85 \cdot 10^{-4}\right] \tag{34}$$

$$k_3 = \left[3.0 \cdot 10^{-6} \ldots 76.5 \cdot 10^{-6}\right]. \tag{35}$$

The parameters k_1 and k_2 remain within a comparably small range. The variations in (33) and (34) can be explained by variations of about a factor of two of the ratio of fan height and fan diameter for different investigated types. The wide variation of k_3 in (35) is due to the mechanical efficiency of the fan. The minimum gap width between fan blade and housing is limited by manufacturing tolerances. With decreasing fan diameter D, the ratio of this gap (where the turbulent losses occur) and the diameter increases in a non-linear way. This results in a non-linear decrease of fan efficiency, and in very large values of k_3 for small fan diameters as compared to larger ones. With the fan laws (29)–(31), assuming $D = c$, and defining

$$\begin{aligned} A_1 &= 10^{-3}\tfrac{k1}{k2} & A_2 &= 5 \cdot 10^{-4}\tfrac{1}{\sqrt{k2}} \\ A_3 &= 6.5\tfrac{\sqrt{k2}}{k1} & A_4 &= 7.5 \cdot 10^{-4}\tfrac{1}{k1} \end{aligned} \tag{36}$$

the three thermal resistance components of the heat sink can be written as

$$R^*_{th,FIN} = \frac{\frac{1}{2\lambda_{HS}L}}{1 - 10^{-3} \cdot \frac{k1}{k2} \cdot \frac{L}{N\,s^2 c}} = \frac{\frac{1}{2\lambda_{HS}L}}{1 - A_1 \cdot \frac{L}{N\,s^2 c}} \tag{37}$$

$$R_{th,conv} = \frac{1.3 \cdot 10^4 \frac{k2}{k1} \frac{s^4}{L^2 c}}{\frac{1}{N} + 2 \cdot 10^3 \cdot \sqrt{k_2} \cdot \frac{s^2 c}{L}} = \frac{A_3 \cdot \frac{s^2}{L\,c^2}}{1 + A_2 \cdot \frac{L}{N\,s^2 c}} \tag{38}$$

$$R_{th,\Delta T} = \frac{7.5 \cdot 10^{-4}}{k_1} \cdot \frac{1}{N\,c^3} = \frac{A_4}{N\,c^3}. \tag{39}$$

D. Optimizing the Cooling System Performance Index

The power density d_{SYS} (kW/litre) of the converter system is defined as

$$d_{SYS} = \frac{P_{OUT,SYS}}{Vol_{SYS}} = \frac{\eta_{SYS}}{1 - \eta_{SYS}} \frac{P_{V,SYS}}{Vol_{SYS}} = \frac{\eta_{SYS}}{1 - \eta_{SYS}} \frac{\Delta T^{max}_{S-a}}{R_{th,S-a}\,Vol_{SYS}} \tag{40}$$

where $P_{OUT,SYS}$ is the output power of the system, Vol_{SYS} the system volume, η_{SYS} its efficiency, $P_{V,SYS}$ its losses, and $\Delta T_{S\text{-}a}$ the difference between the temperatures of the heat sink surface and the ambient. For comparison of different heat sink designs concerning power density, we proposed in [2] and [18] the cooling system performance index (CSPI) (see also [19], published at the same time, and giving results in good agreement with the findings of this paper). We give it here in a slightly modified but equivalent form as

$$CSPI\left[\frac{\mathrm{W}}{\mathrm{K} \cdot \mathrm{litre}}\right] = \frac{G_{th,S\text{-}a}\left[\frac{\mathrm{W}}{\mathrm{K}}\right]}{Vol_{CS}\,[\mathrm{litre}]} \tag{41}$$

where $G_{th,S\text{-}a} = 1/R_{th,S\text{-}a}$ is the thermal conductance of the heat sink. Although the CSPI has units of W/(K·litre), it is intended for use as an index, and as indices are typically given without units, for clarity the use of units next to CSPI figures will be omitted further on in this paper. The cooling system power density d_{CS} (W/litre) can be expressed proportional to $CSPI$ as

$$d_{CS}\left[\tfrac{\mathrm{W}}{\mathrm{litre}}\right] = \frac{P_{OUT,SYS}}{Vol_{CS}} = \frac{\eta_{SYS}}{1 - \eta_{SYS}}\,\Delta T^{max}_{S-a} \cdot CSPI > d_{SYS}. \tag{42}$$

The density d_{CS} considers all components of the cooling system. In case of forced-air cooling this is the heat sink volume plus the fan volume.

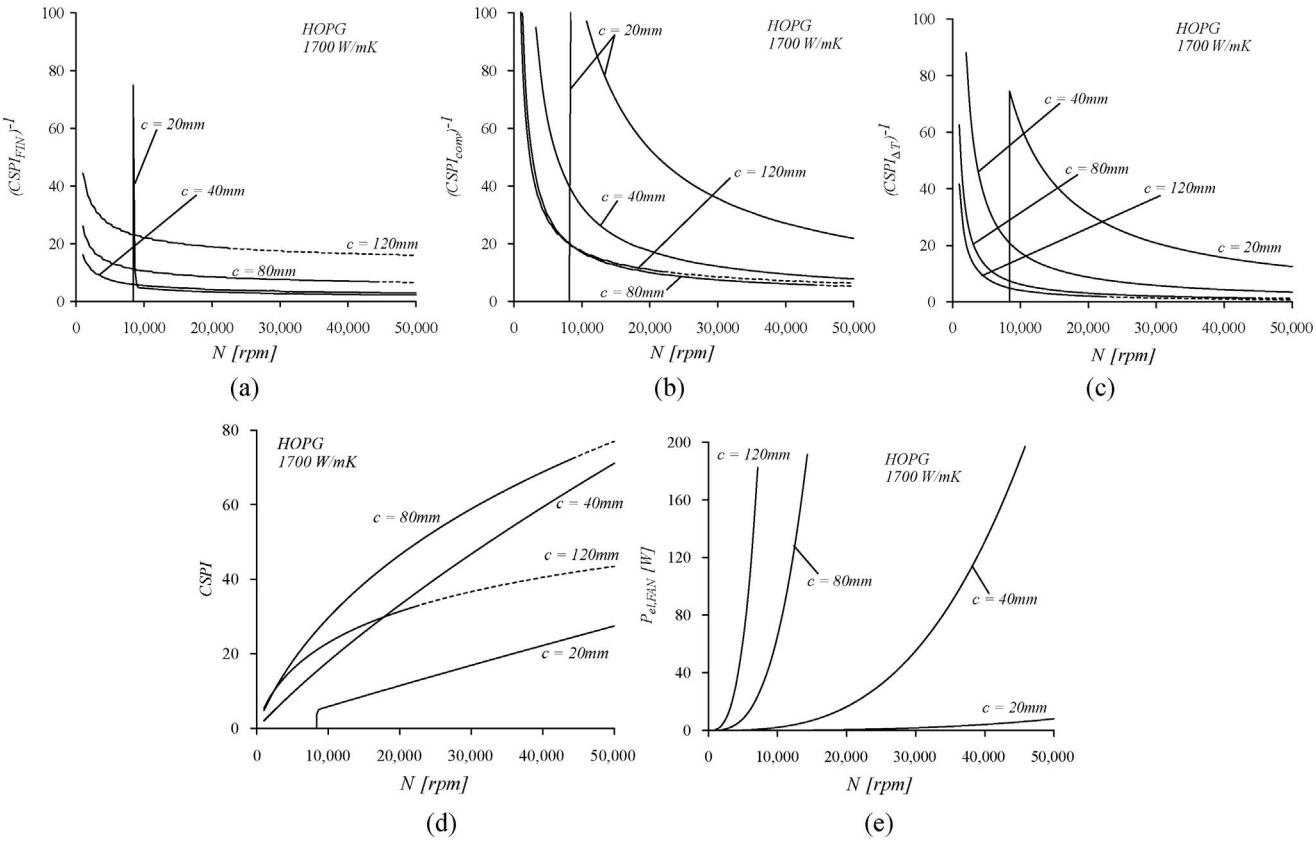

Fig. 4. Variation of fan rotating speed N and different fan diameters, employing heat sink material HOPG with chip area $A_{CHIP} = 32\,\mathrm{cm}^2$. Dotted lines indicate Reynolds numbers higher than 2300, violating the laminar flow condition. Contribution of (a) heat flow through heat sink material, (b) convection and (c) temperature gradient of air in flow direction, (d) resulting CSPI, and (e) necessary fan power.

The CSPI is very useful to directly compare heat sink plus fan combinations of different size, of different types, and in different applications. If an approximate value of CSPI is known, and the maximum allowed thermal resistance of the heat sink is given (from the knowledge of maximum ambient temperature, maximum junction temperature, and maximum semiconductor junction-to-case temperature), the volume of the cooling system of the converter can be directly calculated. This makes it very easy for the electrical engineer to roughly estimate the total volume, mass, and power density of a converter design without any deeper knowledge of the cooling system. For commercial non-optimized heat sinks for converter systems in the kW-range employing forced-air-cooling, the value of CSPI is typically in the range of 3–5 (as shown in [2]). Optimized heat sinks, as will be shown in the following, can reach much higher CSPI-values.

Defining the total chip area to be cooled as

$$A_{CHIP} = L\,c \tag{43}$$

we can, based on the assumption that the fan thickness is approximately one third of its diameter, define

$$\begin{aligned} CSPI^{-1} &= R_{th,S-a}^{(HS)} \cdot Vol_{CS} = (R_{th,FIN}^{*} + R_{th,conv} + R_{th,\Delta T}) \\ &\quad \cdot (L + \tfrac{1}{3}c)\,c^2 \\ &= CSPI_{FIN}^{-1} + CSPI_{conv}^{-1} + CSPI_{\Delta T}^{-1} \end{aligned} \tag{44}$$

assuming that the gap between fan and heat sink is small compared to c and L. This gives the inverse of CSPI as

$$CSPI^{-1} = \frac{\frac{c^2}{2\lambda_{HS}}\,(1+\frac{c^2}{3\,A_{CHIP}})}{1 - A_1 \cdot \frac{A_{CHIP}}{N\,s^2c^2}} + \frac{A_3 \cdot (1+\frac{c^2}{3\,A_{CHIP}})\,s^2}{1+A_2 \cdot \frac{A_{CHIP}}{N\,s^2c^2}} + \frac{A_4 \cdot (\frac{A_{CHIP}}{c^2}+\frac{1}{3})}{N} \tag{45}$$

with the necessary side condition [see (20) and (21)]

$$\sqrt{A_1 \cdot \frac{A_{CHIP}}{N\,c^2}} \;\leq\; s \;\leq\; \sqrt[3]{\frac{A_1}{5} \cdot \frac{A_{CHIP}}{N\,c}}\,. \tag{46}$$

The fin number is

$$n = (int)\left[A_1 \cdot \frac{A_{CHIP}}{N\,s^3 c}\right] \tag{47}$$

and the Reynolds number

$$Re_m = \;\; 6.35 \cdot 10^4 \cdot k_1 \cdot \frac{N\,c^2}{n} \tag{48}$$

must not be significantly larger than 2300 in order to verify the original assumption of laminar or mixed flow in the heat sink channels [15]. For optimization of the CSPI, the optimum channel width has to be found for every parameter set (λ_{HS}, A_{CHIP}, c, N).

Fan rotating speed dependence of the three terms in (45) contributing to the total CSPI is shown in Fig. 4 for heat sink material highly orientated pyrolytic graphite (HOPG). Only the term $(CSPI_{FIN})^{-1}$ [Fig. 4(a)] can be influenced by the

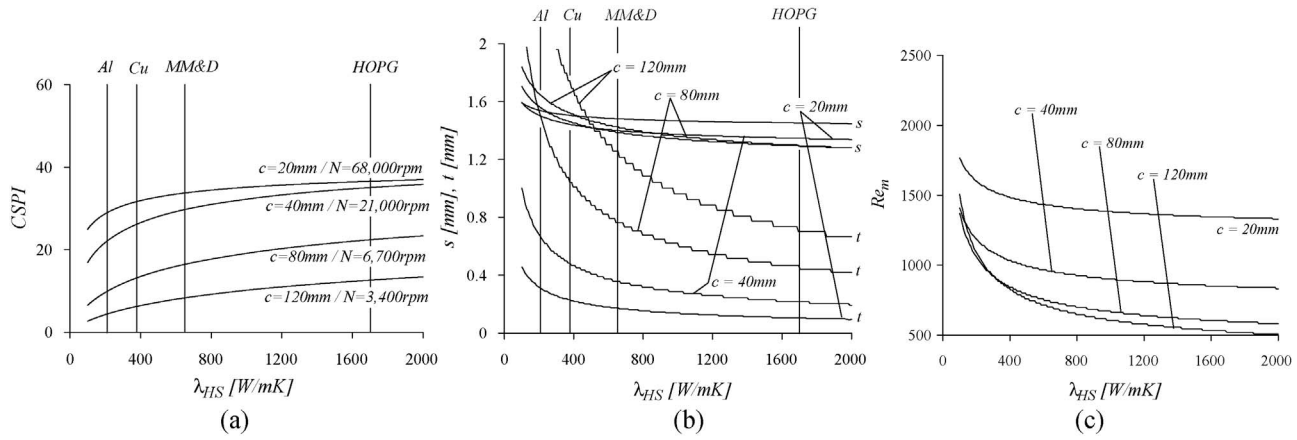

Fig. 5. Variation of thermal conductivity of heat sink material λ_{HS} with $P_{FAN,MAX}$ = 20W and A_{CHIP} = 32 cm^2. (a) Effect on CSPI. (b) Effect on optimal heat sink channel dimensions. (c) Effect on Reynolds number.

heat sink conductivity. Therefore, it only makes sense to invest in advanced materials, if the other two terms, $(CSPI_{conv})^{-1}$ [Fig. 4(b)] and $(CSPI_{DT})^{-1}$ [Fig. 4(c)], are small compared to $(CSPI_{FIN})^{-1}$. For low rotating speed N and small diameter c, the term $(CSPI_{FIN})^{-1}$ will be negative which means there is no design solution with an operating point as defined in (15) and (16). In this example, the chip area A_{CHIP} is set to be 32 cm^2 which is approximately the space needed for all three power modules containing the chips for a 10 kW Vienna Rectifier (VR1).

Theoretically, as shown in Fig. 4(d), there is no limit of the CSPI if the fan rotating speed N is increased. But, as one can immediately see from Fig. 4(e), the power consumption of the fan will reach unrealistically high values. Therefore, by defining the maximum acceptable power consumption $P_{FAN,MAX}$ from (31), the maximum tolerated fan rotating speed can be expressed in terms of the fan diameter $D = c$ as

$$N = \sqrt[3]{\frac{1}{k_3} \cdot P_{FAN}^{\max}} \cdot c^{-5/3} \tag{49}$$

resulting in

$$CSPI^{-1} = CSPI^{-1}(c, \lambda_{HS}, A_{CHIP}, P_{FAN}^{\max}) = Rth_{S-a}^{HS} \cdot Vol_{CS} = \frac{\frac{c^2}{2\lambda_{HS}}\left(1 + \frac{c^2}{3\,A_{CHIP}}\right)}{1 - \frac{A_1 \cdot A_{CHIP}}{s^2 \cdot \sqrt[3]{\frac{1}{k_3} \cdot P_{FAN}^{\max}} \cdot c^{1/3}}} + \frac{A_3 \cdot \left(1 + \frac{c^2}{3\,A_{CHIP}}\right) s^2}{A_2 \cdot A_{CHIP}} + \frac{A_4 \cdot \left(A_{CHIP} + \frac{1}{3}c^2\right)}{\sqrt[3]{\frac{1}{k_3} \cdot P_{FAN}^{\max}} \cdot c^{1/3}} \tag{50}$$

which is dependent only on the thermal conductivity of the heat sink λ_{HS} and the diameter of the fan c. The channel width s has to be always chosen in order to maximize CSPI. Therefore, the channel width s is not an independent design parameter in this equation. Condition (46) has to be fulfilled, and (48) should not be violated.

In Fig. 5, the results of the numerical computation of (50) are shown. The chip area A_{CHIP} is selected to fulfill the specifications of a 10 kW Vienna Rectifier (VR1), and the fan losses

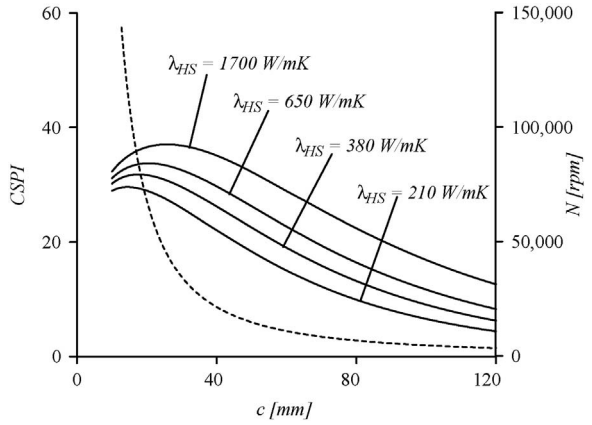

Fig. 6. Variation of c with A_{CHIP} = 32 cm^2 and $P_{FAN,MAX}$ = 20 W.

are limited to 20 W. Fig. 5(a) shows that with increasing λ_{HS} the CSPI becomes flat because only the first term $(CSPI_{FIN})^{-1}$ is affected. Fig. 5(b) shows the fin and channel geometry necessary to realize the optimum heat sink. With larger values of λ_{HS} the fin thickness must be manufactured below 0.5 mm which provides a limit to the practical realization, which will be discussed in the next section. Fig. 5(c) shows that the Reynolds number is always below 2300.

In Fig. 6 (all parameters equal to Fig. 5) fan diameter c is varied. From Figs. 5 and 6, one can see that it is possible for cooling systems of converters in the kW-range to reach a CSPI of about 20 (five times larger than typical commercial heat sinks) by employing aluminum and optimizing fan and heat sink geometry. Employing materials with much higher thermal conductivities does not improve the CSPI correspondingly; as seen in Fig. 6, e.g., c = 40 mm, increasing the thermal conductivity eight times less than doubles the CSPI.

III. Practical Considerations and Experimental Results

In the previous theoretical sections, we did not comment on the many practical difficulties associated with the materials shown in Table I. To name a few well-known problems,

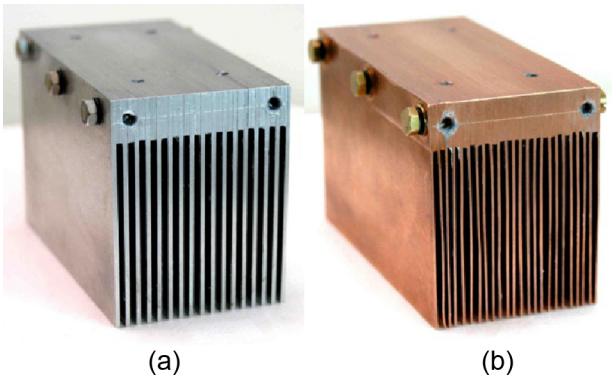

Fig. 7. Optimized heat sink employing SanAce $40 \times 40 \times 28$ mm/50 dB [11] with $b = c = 40$ mm, $d = 10$ mm, $L = 80$ mm, $A_{CHIP} = 32$ cm^2, $Vol_{CS} = 0.22$ liter. (a) Aluminum with $n = 16$, $s = 1.5$ mm, $t = 1.0$ mm. (b) Copper with $n = 23$, $s = 1.3$ mm, $t = 0.5$ mm.

TABLE II
EXPERIMENTAL MEASUREMENTS OF OPTIMIZED HEAT SINKS FOR A 10 KW VIENNA RECTIFIER

Material	Value	R_{th} (K/W)	*CSPI*
Aluminum	Theoretical	0.254	20.0
	Measured	0.260	17.5
Copper	Theoretical	0.240	22.2
	Measured	0.215	21.2

HOPG shows only high thermal conductivity in-plane which is sufficient for the fins but provides very poor heat spreading within the base plate. HOPG is very expensive—according to [12], the material for a prototype as shown in Fig. 7 would cost more than 1000 Euro. Further, employing for example Al-diamond metal-matrix [10], [11] might limit the fin thickness minimum to about 1.0 mm which is far above the calculated optimum [Fig. 5(b)]. For these reasons two optimized heat sinks for a 10 kW-VR1 based on (1)–(14) and/or (50) were manufactured for the purpose of this paper out of more common materials—aluminum and copper. They are shown in Fig. 7. Details concerning the manufacturing, measurements and design tolerances have been published in [13]. The measurements verify the theoretical calculations with very good accuracy and are shown in Table II.

Furthermore, to show the operation of an optimized heat sink, the aluminum heat sink from Fig. 7(a) was observed under load with the use of a thermal imaging camera. Fig. 8 shows a thermal image of the heat sink when a load of 60 W (heat resistor) is mounted on top. The image was taken after the temperature distribution had stabilized (more than 30 min of continuous operation). The hot area in the middle of the heat sink is the middle fixture of the fan, where there is, of course, no direct air flow. In a non-optimized heat sink, according to the theory presented, we would expect the air in the channels to be either just as hot as the fins, or just as cool as the ambient, in either case signifying non-optimal heat transfer. Here however it can be seen from the image in Fig. 8 that the air in the channels is just slightly cooler than the fins, exactly as predicted by the optimization theory presented earlier. This fact tells us that the heat is being efficiently dissipated from the fins into the air, and also, since the air is slightly cooler, that heat is also being removed via the fan.

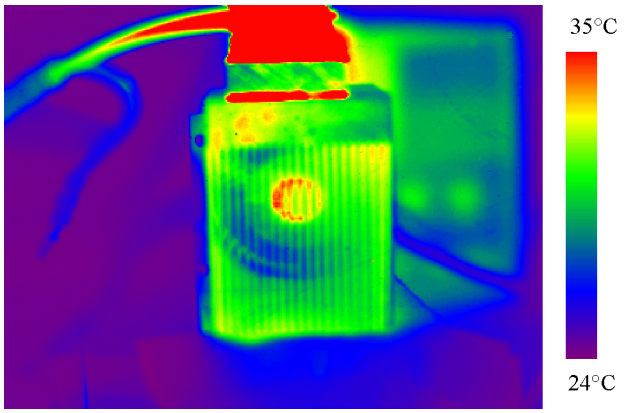

Fig. 8. Thermal image of the aluminum heat sink [Fig. 7(a)] under a load of 60 W (resistor: red block on top). Purple color is the ambient at 24 °C. The bright green of the fins is at 31 °C.

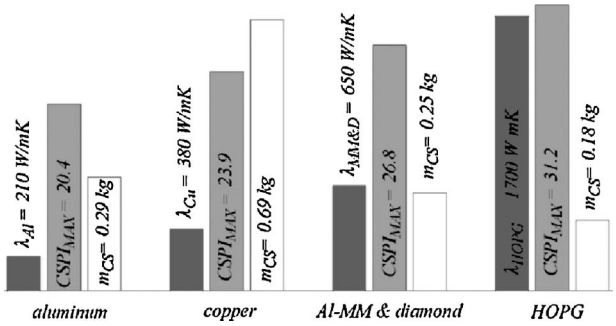

Fig. 9. Comparing different heat sink materials for a 10 kW-VR1.

IV. CONCLUSION

An equation to directly calculate the CSPI that specifies cooling system volume for a given thermal resistance by taking into account thermal conductivity of the heat sink material and fan characteristic was presented. An optimization for a 10 kW converter shows that aluminum might still be a very good choice considering manufacturability, weight, and cost (see Fig. 9). However for different applications and/or design specifications advanced thermal materials might provide significant potential for cooling power electronics. For example, in weight and size-critical applications such as aerospace, HOPG heat sinks could offer superior performance at a smaller weight than with metal heat sinks. Finally, experimental results featuring an optimized heat sink under load were presented, and were found to be in line with the predictions made by the optimization theory presented in this paper.

REFERENCES

[1] S. Lee, "Optimum design and selection of heat sinks," *IEEE Trans. Compon. Packag. Manuf. Technol., Part A*, vol. 18, no. 4, pp. 812–817, Dec. 1995.

[2] U. Drofenik, G. Laimer, and J. W. Kolar, "Theoretical converter power density limits for forced convection cooling," in *Proc. Int. PCIM Eur. Conf.*, Jun. 2005, pp. 608–619.

[3] W. A. Khan, J. R. Culham, and M. M. Yovanovich, "Optimization of microchannel heat sinks using entropy generation minimization method," *IEEE Trans. Compon. Packag. Technol.*, vol. 32, no. 2, pp. 243–251, Jun. 2009.
[4] A. Shah, B. G. Sammakia, and H. Srihari, "A numerical study of the thermal performance of an impingement heat sink-fin shape optimization," *IEEE Trans. Compon. Packag. Technol.*, vol. 27, no. 4, pp. 710–717, Dec. 2004.
[5] P. Ning, G. Lei, F. Wang, and K. D. T. Ngo, "Selection of heatsink and fan for high-temperature power modules under weight constraint," in *Proc. IEEE APEC*, Feb. 2008, pp. 192–198.
[6] W. Leonard, P. Teerstra, J. R. Culham, and A. Zaghol, "Characterization of heatsink flow bypass in plate fin heatsinks," in *Proc. ASME IMECE*, Nov. 2002, pp. 1–8.
[7] C. Zweben, "Revolutionary new thermal management materials," *Electron. Cooling*, vol. 11, no. 2, pp. 36–37, May 2005.
[8] C. Zweben, "Ultrahigh-thermal-conductivity packaging materials," in *Proc. 21st Annu. IEEE Semiconductor Thermal Meas. Manage. Symp.*, Mar. 2005, pp. 168–174.
[9] C. Zweben, "Advanced composites and other advanced materials for electronic packaging thermal management," in *Proc. Int. Symp. Adv. Packag. Mater.: Process, Properties Interfaces*, Mar. 2001, pp. 360–365.
[10] O. Beffort, S. Vaucher, and F. A. Khalid, "On the thermal and chemical stability of diamond during processing of Al/Diamond composites by liquid metal infiltration (squeeze casting)," *Diamond Related Mater.*, vol. 13, no. 10, pp. 1834–1843, Oct. 2004.
[11] A. Khalid, O. Beffort, U. E. Klotz, B. A. Keller, and P. Gasser, "Microstructure and interfacial characteristics of aluminum-diamond composite materials," *Diamond Related Mat.*, vol. 13, no. 3, pp. 393–400, Mar. 2004.
[12] Official Website of Optigraph GmbH. (2006, Mar.) [Online]. Available: http://www.optigraph.fta-berlin.de/optigraph.html
[13] U. Drofenik and J. W. Kolar, "Sub-optimum design of a forced air cooled heat sink for simple manufacturing," in *Proc. 4th PCC*, Apr. 2007, pp. 1189–1194.
[14] U. Drofenik, G. Laimer, and J. W. Kolar, "Pump characteristic based optimization of a direct water cooling system for a 10 kw/500 kHz Vienna rectifier," *IEEE Trans. Power Electron.*, vol. 20, no. 3, pp. 704–714, May 2005.
[15] H. D. Baehr and K. Stephan, *Wärme- und Stoffübertragung*, 3rd ed. Berlin, Germany: Springer-Verlag, 1998.
[16] Official Website of Sanyo Denki Co., Ltd. (2006, Mar.) [Online]. Available: http://www.sanyodenki.co.jp
[17] S. L. Dixon, *Fluid Mechanics and Thermodynamics of Turbomachinery*, 4th ed. Oxford, U.K.: Butterworth-Heinemann, 1998.
[18] U. Drofenik and J. W. Kolar, "Analyzing the theoretical limits of forced air-cooling by employing advanced composite materials with thermal conductivities > 400 W/mK," in *Proc. 4th Int. CIPS*, Jun. 2006, pp. 323–328.
[19] M. F. Holahan, "Fins, fans, and form: Volumetric limits to air-side heatsink performance," *IEEE Trans. Compon. Packag. Technol.*, vol. 28, no. 2, pp. 255–262, Jun. 2005.

Uwe Drofenik (S'96–M'00) was born in Moedling, Austria, in 1970. He received the M.S. (cum laude) and Ph.D. (cum laude) degrees in electrical engineering from the Vienna University of Technology, Vienna, Austria, in 1995 and 1999, respectively.

From 1997 to 2000, he was a Scientific Assistant with the Vienna University of Technology, where he was involved in power electronic projects and CAD/CAM software development for industry. In 2001, he joined the Swiss Federal Institute of Technology Zurich, Zurich, Switzerland, as a Post-Doctoral Researcher, where he is heading the development of a multi-disciplinary simulation software for "virtual prototyping in power electronics." This includes the development, programming, and experimental testing of numerical circuit simulators, thermal and electromagnetic 3D-FEM simulators, algorithms for predicting reliability and life time of electronic components and systems, and the intelligent coupling of all these software-modules within a single design-platform. He is the author of the web-based interactive educational power-electronics software iPES (www.ipes.ethz.ch). In 1996, he was a Researcher with the Masada-Ohsaki Laboratory, University of Tokyo, Tokyo, Japan. He has published more than 50 conference and journal papers and four patents.

Dr. Drofenik received the "Isao Takahashi Award for Outstanding Achievement in Power Electronics" from the IEE of Japan in 2005. He is a member of the Austrian Society of Electrical Engineering.

Andrija Stupar (S'02) was born in Belgrade, Serbia, in 1984. He received the Bachelors (with honors) and Masters degrees from the University of Toronto, Toronto, ON, Canada, where he worked on the design and implementation of digital controllers for low-power switch-mode power supplies. He is currently pursuing the Ph.D. degree from the Power Electronic Systems Laboratory, Swiss Federal Institute of Technology Zurich, Zurich, Switzerland, with research focusing on reliability, thermal modeling, and optimization.

Johann W. Kolar (M'89–SM'04–F'10) received the M.S. and Ph.D. (summa cum laude/promotio sub auspiciis praesidentis rei publicae) degrees from the University of Technology Vienna, Vienna, Austria.

Since 1984, he has been an Independent International Consultant in close collaboration with the University of Technology Vienna, in the fields of power electronics, industrial electronics, and high performance drives. He has proposed numerous novel pulse width modulated converter topologies and modulation and control concepts, e.g., the VIENNA rectifier and the three-phase AC-AC sparse matrix converter. He has published over 350 scientific papers in international journals and conference proceedings, and has filed 75 patents. He was appointed the Professor and Head of the Power Electronic Systems Laboratory, Swiss Federal Institute of Technology (ETH) Zurich, Zurich, Switzerland, on Feb. 1, 2001. The focus of his current research is on AC-AC and AC-DC converter topologies with low effects on the mains, e.g., for power supply of data centers, more-electric-aircraft, and distributed renewable energy systems. Further main areas of his research include the realization of ultracompact and ultraefficient converter modules employing latest power semiconductor technology (e.g., SiC), novel concepts for cooling and electromagnetic interference filtering, multidomain/scale modeling/simulation and multiobjective optimization, physical model-based lifetime prediction, pulsed power, and ultrahigh speed and bearingless motors.

Dr. Kolar received the Best Transactions Paper Award from the IEEE Industrial Electronics Society in 2005, the Best Paper Award from the ICPE in 2007, the 1st Prize Paper Award from the IEEE IAS IPCC in 2008, the IEEE IECON Best Paper Award from the IES PETC in 2009, the 2009 IEEE Power Electronics Society Transaction Prize Paper Award, and the 2010 Best Paper Award of the IEEE/ASME TRANSACTIONS ON MECHATRONICS. He received an Erskine Fellowship from the University of Canterbury, Christchurch, New Zealand, in 2003. He initiated and/or is the Founder/Co-Founder of four spin-off companies targeting ultrahigh speed drives, multidomain/level simulation, ultracompact/efficient converter systems, and pulsed power/electronic energy processing. In 2006, the European Power Supplies Manufacturers Association awarded the Power Electronics Systems Laboratory of ETH Zurich as the leading academic research institution in power electronics in Europe. He is a member of the IEEJ and of the international steering committees and technical program committees of numerous international conferences in the field (e.g., Director of the Power Quality Branch of the International Conference on Power Conversion and Intelligent Motion). He is the Founding Chairman of the IEEE PELS Austria and Switzerland Chapter and the Chairman of the Education Chapter of the EPE Association. From 1997 to 2000, he was an Associate Editor of the IEEE TRANSACTIONS ON INDUSTRIAL ELECTRONICS and, since 2001, has been an Associate Editor of the IEEE TRANSACTIONS ON POWER ELECTRONICS. Since 2002, he has been an Associate Editor of the *Journal of Power Electronics* of the Korean Institute of Power Electronics and a member of the Editorial Advisory Board of the *IEEJ Transactions on Electrical and Electronic Engineering*.